SCIENCE CHINA
Information Sciences

• RESEARCH PAPER •

September 2025, Vol. 68, Iss. 9, 190306:1–190306:16
https://doi.org/10.1007/s11432-024-4477-4

Special Topic: Cohesive Clustered Satellites System for 5GA and 6G Networks

Modeling and analysis of satellite-terrestrial covert communications

Hao SHI[1], Na DENG[1*], Bo LI[2], Haichao WEI[3], Weidang LU[4] & Nan ZHAO[1]

[1]*School of Information and Communication Engineering, Dalian University of Technology, Dalian 116024, China*
[2]*School of Information Science and Engineering, Harbin Institute of Technology (Weihai), Weihai 264209, China*
[3]*School of Information Science and Technology, Dalian Maritime University, Dalian 116024, China*
[4]*College of Information Engineering, Zhejiang University of Technology, Hangzhou 310023, China*

Received 22 November 2024/Revised 19 March 2025/Accepted 4 June 2025/Published online 15 August 2025

Abstract The low Earth orbit (LEO) satellite-terrestrial covert communication is one of the most promising research areas to provide security for seamless global communication. In this paper, we consider downlink LEO satellite-terrestrial covert communication networks, where the interference nodes follow a Poisson point process distributed in the terrestrial plane and the space-terrestrial fading is modeled by the Shadowed-Rician fading. The main concern is how to utilize the interference uncertainty and channel uncertainty to hide the communication behavior, thereby avoiding the detection of Willie and ensuring the satellite-terrestrial communication reliability in three distinct network models: (i) the satellite located at a fixed position, (ii) the satellite moving along its orbit, and (iii) the satellite randomly distributed in its visible orbit. We derive the analytical expressions for false alarm, missed detection, and connection probability for the three network models. To obtain the covert throughput, which comprehensively accounts for the covertness and reliability, we formulate an optimization problem and propose a one-dimensional search method to solve an equivalent problem. Finally, simulations validate the accuracy of the derived theoretical expressions and demonstrate the impact of various parameters on system performance.

Keywords satellite-terrestrial covert communication, covert probability, covert throughput

Citation Shi H, Deng N, Li B, et al. Modeling and analysis of satellite-terrestrial covert communications. Sci China Inf Sci, 2025, 68(9): 190306, https://doi.org/10.1007/s11432-024-4477-4

1 Introduction

1.1 Motivation

With the ever-increasing demand for seamless coverage and ubiquitous connectivity, satellite communication has drawn significant attention from both academia and industry due to its rapidly progressive development in recent years [1]. Due to the unparalleled potential for various communication scenarios, satellites can provide direct links for remote areas, act as relays for long-distance communications, and serve as the complements for dense terrestrial networks. Satellite systems are primarily categorized into three types: geostationary Earth orbit (GEO), medium Earth orbit (MEO), and low Earth orbit (LEO). Among them, LEO satellites have become a paramountly promising research area due to the low transmission delay and minimal signal attenuation, while limited coverage resulting from low altitude promotes multiple satellites to work together and form a constellation [2–4]. For example, Space X proposed a LEO satellite constellation project Starlink and planned to launch 42000 satellites to provide space service. However, satellite communication is more vulnerable in terms of information security than terrestrial communication. Besides the common natures of channel openness and signal broadcast, satellite communication introduces new threat features, such as long transmission distance, extensive coverage, and specific orbit, which increase the number of potentially malicious devices [5].

Encryption and physical layer security (PLS) are traditionally used to secure communication [6]. However, the former consumes excessive computation resources, which are scarce on satellites, while the latter requires accurate channel state information (CSI), which is difficult to obtain for the satellite due to its high mobility. Meanwhile, both focus on protecting the specific information of signals, which is

* Corresponding author (email: dengna@dlut.edu.cn)

invalid against malicious devices with powerful computing capabilities. Furthermore, the attacks may be independent of the specific content and launched when the malicious devices detect the communication behavior. Therefore, it is extremely urgent and challenging to study other technologies to safeguard the security of satellite communication [7]. The emerging covert communication completes the secure information transmission by introducing randomness to conceal the signal into the environment and distort the judgment of the warden [8–11]. Compared to encryption and PLS, their limitations for satellite communication can even be transformed into advantages for covertness. Specifically, covert communication only requires minimal resources for signal processing overhead in terms of energy consumption and can exploit greater spatial randomness introduced by high mobility to evade the detection of the warden [12]. It is important to note that covert communication also requires CSI. However, covert communication can be applied under the more relaxed CSI requirements and even leverage channel uncertainty to enhance the covertness. While numerous studies have contributed to the performance of LEO satellite communication, research on covert communications still remains in its infancy. Thus, it is vital to investigate the LEO satellite-terrestrial covert communication to facilitate commercialization and further research. In this paper, we focus on building various LEO satellite-terrestrial covert communication models and analyzing the fundamental performance metrics, and facilitating further satellite communication design.

1.2 Related work

The rise of covert communication originates from [13], where the authors utilized the information theory to demonstrate that Alice can reliably transmit at most $\mathcal{O}(\sqrt{n})$ bits over n channel uses, which is also known as square root law (SRL). SRL yields a pessimistic conclusion that the reliably transmitted data approach zero when n is sufficiently large. Fortunately, numerous studies have proven that positive covert rate can be achieved when there exists environmental randomness, such as noise, channel fading, and interference [14–16]. Environmental randomness misleads the judgment of the warden, rendering it difficult to distinguish between noise and legitimate signals, thereby enhancing information security. The work of [17] analyzed the impact of interference nodes on covert communication with the tools of stochastic geometry. The authors assumed that interference nodes follow a Poisson point process (PPP) and derived an interesting conclusion that the transmission power and density of interference nodes have no impact on the covert throughput of terrestrial covert communication. In [18], the authors studied covert communication in wireless energy harvesting enabled device-to-device networks. By modeling the power beacons as a PPP and dividing a time slot into two sub-slots, i.e., the energy transmission sub-slot and covert transmission sub-slot, the authors formulated an optimization problem to maximize covert throughput and solved it by alternating optimization. The authors in [19] designed different beamforming schemes to investigate millimeter wave covert communication with finite blocklength, where the wardens are randomly distributed around the legitimate receiver. The results indicate that the performance may degrade with increasing blocklength and further decline with higher warden density. Moreover, many studies focus on applying advanced technologies to covert communication to improve covertness, such as intelligent reflecting surfaces (IRS) [20–24] and unmanned aerial vehicles [25–27].

For satellite communication, there have been numerous studies to investigate their performance from various aspects. The article of [28] utilized stochastic geometry to model the satellite networks as a binomial point process (BPP) and derived the distribution of visible serving distances. Based on the Laplace transform of the interference, the coverage probability and average achievable rate are analyzed. Furthermore, the study defined a new parameter, the effective number of satellites, to compensate for the performance gap between the random network model and the actual one. In [29], the authors investigated the terahertz (THz) LEO satellite-airplane networks, where satellites are distributed on a spherical surface as a BPP. The study analyzed the unique benefits of THz with and without molecular absorption noise, derived the coverage probability and average achievable rate, and concluded that there exists an optimal satellite number to balance the competitive coverage and rate. The authors of [30] investigated the downlink LEO communication networks, analyzed the distance distribution of serving satellites, and proposed a communication throughput maximization problem, which is solved by the developed iterative algorithm. Most notably, the authors considered more practical Shadowed-Rician (SR) fading for satellite links. The work of [31] modeled LEO satellite communication for Internet of Things devices in two different communication scenarios, direct communication and indirect communication aided by gateways, and analyzed their corresponding uplink performance. Furthermore, the authors employed Rayleigh and SR fading for terrestrial and satellite links, respectively.

There is little comprehensive research on satellite-terrestrial covert communication [32,33]. Specifically, the article of [32] proposed an IRS-aided covert satellite-terrestrial communication network and formulated a max-min rate problem to optimize the performance of the system. To deal with the non-convex problem, the authors developed an alternating optimization algorithm by optimizing the transmission power and the reflecting coefficients. And the results demonstrate the significant gains provided by the IRS. In [33], the authors focused on large-scale multi-layer LEO satellite covert communication. In order to model the real conflict between the various roles, the authors constructed a two-stage Stackelberg game and developed an algorithm based on successive convex approximation and golden-section search to achieve the Stackelberg balance.

However, the aforementioned studies did not consider the impact of some practical and key factors. Specifically, the high mobility of satellites yields the inherent spatial randomness and the temporal variation, and numerous wireless devices are located around the legal and illegal terrestrial receivers to produce interference uncertainty, both of which will affect the reliability and covertness of the information transmission. Accordingly, it is imperative to establish accurate network models and conduct fundamental performance analysis for satellite-terrestrial covert communication.

1.3 Contributions

The primary objective of this paper is to provide an analytical framework for the proposed satellite-terrestrial covert communication networks by deriving the expressions of two critical metrics, including covert probability and connection probability, and analyzing the covert throughput. The major contributions of this paper are summarized as follows.

- We mainly focus on satellite-terrestrial covert communication networks, where a single satellite as Alice transmits covert signals to terrestrial Bob while the communication is affected by terrestrial interference nodes, which follow a PPP. We propose three network models: the satellite located at a fixed position, the satellite moving along its orbit, and the satellite distributed in its visible orbit randomly. The first model is the fundamental model as a reference baseline for subsequent models. The second model is a time-varying model that realistically reflects covert performance during movement, and the third one is the statistical model for a comprehensive statistical analysis.
- We derive covert probability and connection probability for the proposed three network models and formulate an optimization problem to obtain covert throughput. Then we simplify the problem by analyzing the relationship between the variables and the constraints and solve it by one-dimension search.
- We provide simulations to validate the analytical expressions and investigate the impact of various system parameters on covert probability and connection probability. The results indicate that the satellite moving along its orbit can provide greater reliability but worse covertness compared to the satellite randomly distributed in its visible orbit. Additionally, severe channel shadowing will diminish the received signal power quality while enhancing the covertness by introducing channel uncertainty.

1.4 Organization

The remainder of this paper is organized as follows. Section 2 introduces the network models, the detection strategy of Willie, and the classic covert performance metrics. Section 3 derives the general expressions of covert probability and connection probability for the three network models. Section 4 formulates an optimization problem to obtain the covert throughput and gives its solution correspondingly. Section 5 presents the analytical result and validates it by simulations. Finally, Section 6 gives the conclusion.

2 System model

In this section, we first propose three LEO satellite-terrestrial covert communication network models: fixed distance model (FDM), moving distance model (MDM), and statistical distance model (SDM), and further demonstrate the communication model with the expressions of the received signal and the signal-to-interference ratio (SIR) of Bob. Then, we elaborate on the detection strategy to obtain the optimal detection capability for Willie. Finally, we present the metrics to evaluate the performance of covert communication, including the connection probability as a measure of reliability, the covert probability as an indicator of covertness, and the covert throughput that considers both aspects.

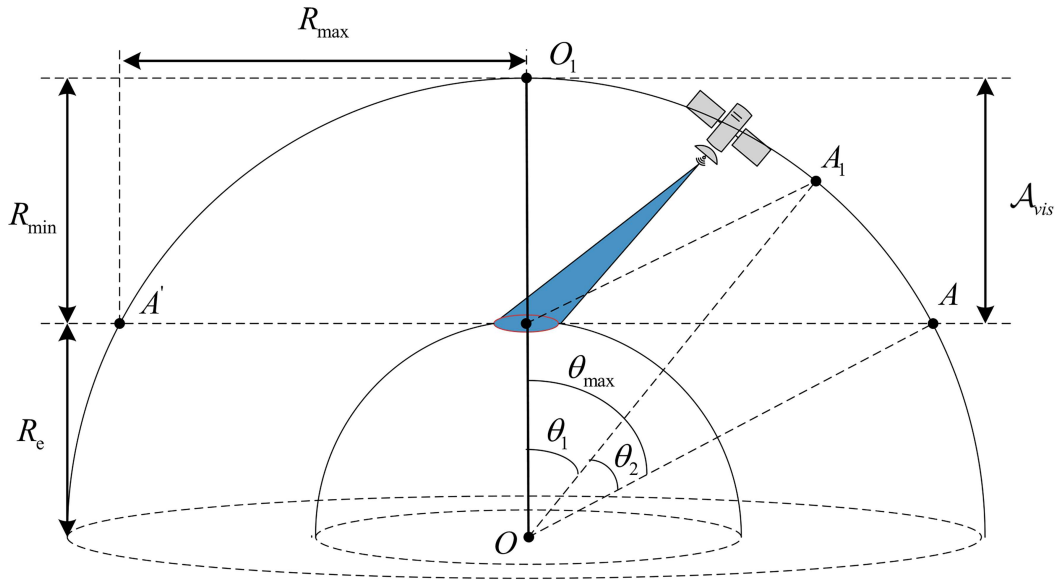

Figure 1 (Color online) Satellite-terrestrial covert communication model with terrestrial interference.

2.1 Network models

As shown in Figure 1, we consider a satellite-terrestrial covert communication network, where a satellite transmitter (Alice) communicates with a terrestrial receiver (Bob) while the warden (Willie) near Bob detects the communication behavior. A satellite can establish a direct link with the terrestrial user when it is above the user's horizon, while the direct link is obstructed by the Earth when below the user's horizon. We define the former orbit as $\mathcal{A}_{\text{vis}}$, which means the satellite in this orbit is visible to the user. Meanwhile, the terrestrial device is surrounded by interfering nodes at the same plane, and the interference signals disrupt the judgment of Willie and decrease the quality of the received signal at Bob. We assume that the terrestrial interfering nodes follow a two-dimensional homogeneous PPP Φ_{I} with the density λ_{I}. The Earth radius, the satellite altitude, and the distance between Alice and terrestrial node o are denoted by R_{e}, $R_{\min}$, and R_o, where $o \in \{b, w\}$, b denotes Bob, and w denotes Willie. Referring to Figure 1, we can calculate the maximum transmission distance $R_{\max} = \sqrt{2R_{\text{e}}R_{\min} + R_{\min}^2}$ by trigonometry. Actually, the satellite is positioned above o when $R_o = R_{\min}$ and located at the intersection of the horizon and the orbit when $R_o = R_{\max}$. Then, we introduce the following three network models.

(1) FDM: In this model, we assume that Alice is located at the fixed position in $\mathcal{A}_{\text{vis}}$. Since satellites constantly move at high speeds along the orbit, this model seems an impossible situation in satellite communication. However, FDM can be applied to scenarios where the relative positions of the satellite and the terrestrial devices remain constant, or the relative position change can be neglected. Typical applications are geostationary Earth orbit satellite communication or short-time communication within a few seconds. Furthermore, FDM can be considered a snapshot of MDM and SDM and act as a theoretical baseline to analyze the impact of mobility and randomness.

(2) MDM: The satellite moves along the orbit at high speed v and attempts to communicate with Bob covertly when it comes into $\mathcal{A}_{\text{vis}}$ in MDM. Since the satellite is constantly moving, R_o will change over time, which is the most essential difference from FDM. This model is realistic for satellite-terrestrial covert communication and applicable to satellites with known deterministic orbits or predictable trajectories.

(3) SDM: Due to the mobility of satellites and the spatial uncertainty of terrestrial receiving nodes, the satellite exhibits random spatial variability from the perspective of terrestrial nodes. Thus, this model assumes that the satellite is randomly distributed in $\mathcal{A}_{\text{vis}}$, which considers the position uncertainty of satellites and is suitable for complex satellite communication scenarios.

Note that in space-terrestrial models, the channel fading is mainly dominated by the line-of-sight path due to fewer obstacles. Furthermore, it has been demonstrated that SR fading is the most accurate channel fading model for space-terrestrial links [30, 31, 34]. Let g_o denote the channel fading between

Alice and o. Then, the cumulative distribution function (CDF) of g_o is

$$F_{g_o}(x)=\Big(\frac{2b_0m}{2b_0m+\Omega}\Big)^m\sum_{z=0}^{\infty}\frac{(m)_z}{z!\Gamma(z+1)}\Big(\frac{\Omega}{2b_0m+\Omega}\Big)^z\gamma\Big(z+1,\frac{1}{2b_0}x\Big),\tag{1}$$

where b_0, m, and Ω are parameters of SR fading. $\gamma(\cdot,\cdot)$ is the lower incomplete gamma function. However, the expression is still in a complex form due to the combination of infinite series and incomplete gamma. For tractable analysis, we adopt the same approximation as [31,34] and approximate the complicated SR fading to the simple Gamma distribution, namely $F_{g_o}(x)\approx\frac{1}{\Gamma(\kappa_s)}\gamma(\kappa_s,\frac{x}{\beta_s})$, where $\kappa_s=\frac{m(2b_0+\Omega)^2}{4mb_0^2+4mb_0\Omega+\Omega^2}$ and $\beta_s=\frac{4mb_0^2+4mb_0\Omega+\Omega^2}{m(2b_0+\Omega)}$ are the shape and scale parameters, respectively. We mainly focus on the interference-limited networks and assume that the terrestrial interference links follow Rayleigh fading. Let $P_{\rm I}$ and P_s denote the transmission power of terrestrial interference nodes and the satellite transmission power. When Alice transmits covert signals, the received signal at Bob is

$$y_b[n]=\sqrt{P_sg_bR_b^{-2}}s_0[n]+\sum_{k\in\Phi_{\rm I}}\sqrt{P_{\rm I}h_{kb}r_{kb}^{-\alpha}}s_k[n],\tag{2}$$

where h_{kb} and r_{kb} represent the channel fading and Euclidean distance between interference node k and Bob with $k\in\Phi_{\rm I}$. α is the path loss exponent of terrestrial links. And we assume that all signals are independent and identically distributed (i.i.d.), i.e., $\mathbb{E}[s_ms_n]=0$ when $m\neq n$ and $\mathbb{E}\left[s_m^2\right]=1$, where $m,n\in[\{0\}\cup\Phi_{\rm I}]$. Based on the above assumptions, the SIR at Bob is expressed as

$$\mathrm{SIR}_b=\frac{P_sg_bR_b^{-2}}{\sum_{k\in\Phi_{\rm I}}P_{\rm I}h_{kb}r_{kb}^{-\alpha}}.\tag{3}$$

2.2 Detection strategy of Willie

To ensure the success of covert communication, it is essential to consider the worst-case case, which means that Willie may know all necessary communication information about the network, such as channel fading, transmission power, and distance, to develop the optimal detection strategy. Willie has the following hypothesis:

$$\begin{aligned}&\mathcal{H}_0:y_w[n]=\sum_{k\in\Phi_{\rm I}}\sqrt{P_{\rm I}h_{kw}r_{kw}^{-\alpha}}s_k[n],\\&\mathcal{H}_1:y_w[n]=\sqrt{P_sg_wR_w^{-2}}s_0[n]+\sum_{k\in\Phi_{\rm I}}\sqrt{P_{\rm I}h_{kw}r_{kw}^{-\alpha}}s_k[n],\end{aligned}\tag{4}$$

where h_{kw} and r_{kw} represent the channel fading and Euclidean distance between interference node k and Willie, $\mathcal{H}_0$ is the null hypothesis that represents the absence of covert communication and $\mathcal{H}_1$ is the alternative hypothesis that represents the occurrence of communications. Given the widespread employment of radiometers in [17,18,20,23], we also adopt it as the Willie's detector. Due to the i.i.d. of signals and $\mathcal{T}_N=\frac{1}{N}\sum_{n=1}^{N}|y_w[n]|^2$, we obtain the following average received signal power at Willie:

$$\mathcal{T}_N=\begin{cases}I_w, & \mathcal{H}_0,\\ S_w+I_w, & \mathcal{H}_1,\end{cases}\tag{5}$$

where $I_w=\sum_{k\in\Phi_{\rm I}}P_{\rm I}h_{kw}r_{kw}^{-\alpha}$ denotes the terrestrial interference power and $S_w=P_sg_wR_w^{-\alpha}$ denotes the received signal power. Willie will make binary decisions based on the rule $\mathcal{T}_N\underset{\mathcal{D}_0}{\overset{\mathcal{D}_1}{\gtrless}}\tau$, where τ is the detection threshold, $\mathcal{D}_1$ indicates that Willie thinks Alice is transmitting, and $\mathcal{D}_0$ represents that Alice is mute. Moreover, Willie will make false alarm (FA) and missed detection (MD) mistakes. Specifically, FA is that Willie makes the wrong decision $\mathcal{D}_1$ when $\mathcal{H}=\mathcal{H}_0$ and MD refers to the decision $\mathcal{D}_0$ when $\mathcal{H}=\mathcal{H}_1$. The FA and MD probabilities are expressed as

$$\mathbb{P}_{\rm FA}=\mathbb{P}(\mathcal{D}_1|\mathcal{H}_0)=\mathbb{P}(\mathcal{T}_N\geqslant\tau|\mathcal{H}_0),\tag{6a}$$

$$\mathbb{P}_{\rm MD}=\mathbb{P}(\mathcal{D}_0|\mathcal{H}_1)=\mathbb{P}(\mathcal{T}_N<\tau|\mathcal{H}_1).\tag{6b}$$

2.3 Covert performance metrics

In this subsection, we focus on the covert communication performance metrics, including connection probability $\mathbb{P}_{\text{con}}$, covert probability ξ, and covert throughput η. Connection probability or covert probability can only reflect the reliability or covertness of the communication, respectively. Covert throughput is a comprehensive metric that integrates the connection probability, covert probability, and transmission rate.

(1) Connection probability: Connection probability $\mathbb{P}_{\text{con}}$ represents the reliability of the communication. If the received transmission rate is less than the preset threshold R_{T}, it is difficult for the receiver to decode the meaningful information from the signal, resulting in the communication outage. Thus, the connection probability is given by

$$\mathbb{P}_{\text{con}} = \mathbb{P}\left(\log\left(1+\text{SIR}_b\right) \geqslant R_{\text{T}}\right). \tag{7}$$

Moreover, it can be observed that P_s and $\mathbb{P}_{\text{con}}$ are positively correlated from their definition. Connection probability is used to measure the likelihood that the system meets communication requirements successfully. However, it only measures reliability without considering covertness, which is crucial for covert communication. Therefore, it is necessary to investigate covertness metrics.

(2) Covert probability: Covert probability ξ is a classic metric for evaluating communication covertness. From the perspective of Alice, it is expected that Willie makes erroneous decisions consistently, generating $\mathcal{D}_1$ when Alice is silent and $\mathcal{D}_0$ when Alice is transmitting. Thus, the general expression of covert probability for an arbitrary detection threshold τ is

$$\xi = \mathbb{P}_{\text{FA}}\left(\tau\right) + \mathbb{P}_{\text{MD}}\left(\tau\right). \tag{8}$$

To ensure the success of covert communication under the worst-case case, we assume that Willie can find the optimal detection threshold τ^* that results in the lowest covert probability, which must also meet covert requirements. The covert probability constraint is

$$\xi^* = \mathbb{P}_{\text{FA}}\left(\tau^*\right) + \mathbb{P}_{\text{MD}}\left(\tau^*\right) \geqslant 1-\varepsilon, \tag{9}$$

where ε represents the covert constraint.

(3) Covert throughput: Covert throughput η reflects the optimal communication performance that can be achieved while satisfying the covertness requirement [17–20]. Specifically, η refers to the maximum achievable throughput under the covert probability constraint and accounts for the connection probability, covert probability, and transmission rate, given by

$$\begin{aligned} \max_{R_{\text{T}}} \quad & \eta = R_{\text{T}}\mathbb{P}_{\text{con}}, \\ \text{s.t.} \quad & \xi^* \geqslant 1-\varepsilon. \end{aligned} \tag{10}$$

Note that Eq. (10) is a fundamental problem, and other constraints may be needed in various models.

3 Covertness and reliability analysis

3.1 FDM

This subsection analyzes the performance of FDM. It is crucial to highlight that this model is static nodes communicating in essence. However, the rapid movement of satellites renders such an assumption unfeasible in satellite communication, but it is vital to our further study on MDM and SDM. We will give the analytical expressions of FA, MD, and connection probability in the following.

Theorem 1. The expression of covert probability in FDM is

$$\xi_1 = \frac{1}{2} + \frac{1}{\pi}\int_0^{+\infty} \frac{\sin(v^\delta B - v\tau)}{v\exp(v^\delta C)}\mathrm{d}v + \frac{\gamma(\kappa_s, s_w\tau)}{2\Gamma(\kappa_s)} - \frac{s_w^{\kappa_s}}{2\pi\Gamma(\kappa_s)}\int_0^{+\infty} \frac{\Upsilon(v)+\Upsilon^*(v)}{v\exp(v^\delta C)}\mathrm{d}v, \tag{11}$$

where $s_w = \frac{R_w^2}{P_s\beta_s}$, $\Upsilon(v) = [\sin(v^\delta B - v\tau) + \mathrm{i}\cos(v^\delta B - v\tau)](s_w+\mathrm{i}v)^{-\kappa_s}\gamma(\kappa_s, (s_w+\mathrm{i}v)\tau)$, $\delta = \frac{2}{\alpha}$, $B = \pi\lambda_{\text{I}}P_{\text{I}}^\delta\frac{\sin\left(\frac{\pi}{2}\delta\right)}{\text{sinc}(\delta)}$, $C = \pi\lambda_{\text{I}}P_{\text{I}}^\delta\frac{\cos\left(\frac{\pi}{2}\delta\right)}{\text{sinc}(\delta)}$, and i is the imaginary unit.

Proof. Considering the definition in (6a), we first derive FA as

$$\mathbb{P}_{\mathrm{FA}} = 1 - F_{I_w}(\tau), \tag{12}$$

where $F_{I_w}(\cdot)$ is the CDF of I_w. Since there have been comprehensive studies of terrestrial interference with a PPP, we omit complex derivations and directly apply corresponding results. Based on the Gil-Pelaez inversion theorem, Laplace transforms, and the formula derivation from [18], the CDF of terrestrial interference signal power I_o is

$$F_{I_o}(x) = \frac{1}{2} - \frac{1}{\pi}\int_0^{+\infty} \frac{\sin(v^\delta B - vx)}{v\exp(v^\delta C)}\mathrm{d}v, \tag{13}$$

where $o \in \{b, w\}$, b denotes Bob, and w denotes Willie. Therefore, we have

$$\mathbb{P}_{\mathrm{FA}} = \frac{1}{2} + \frac{1}{\pi}\int_0^{+\infty} \frac{\sin(v^\delta B - v\tau)}{v\exp\left(v^\delta C\right)}\mathrm{d}v. \tag{14}$$

Note that the three network models have the same mathematical expressions of FA due to identical interference distribution. Then, we derive the probability of MD according to (6b), given by

$$\mathbb{P}_{\mathrm{MD1}} = \mathbb{P}(I_w + S_w \leqslant \tau) = \int_0^{\tau} F_{I_w}(\tau - x) f_{S_w}(x)\mathrm{d}x, \tag{15}$$

where f_{S_w} is the PDF of the received satellite signal power S_w. From the definition of CDF, we have

$$F_{S_o}(x) = \mathbb{P}(S_o \leqslant x) = \mathbb{P}\Big(g_o \leqslant \frac{xR_o^2}{P_s}\Big) = F_{g_o}\Big(\frac{xR_o^2}{P_s}\Big). \tag{16}$$

Then we can derive the PDF of S_o by substituting the aforementioned channel fading approximation $g_o \sim \mathrm{Gamma}(\kappa_s, \beta_s)$ and taking the derivative with respect to x in (16), given by

$$f_{S_o}(x) = \frac{\partial}{\partial x}\Big(F_{g_o}\Big(\frac{xR_o^2}{P_s}\Big)\Big) = \frac{R_o^2}{P_s} f_{g_o}\Big(\frac{xR_o^2}{P_s}\Big) = \frac{s_o^{\kappa_s}}{\Gamma(\kappa_s)} x^{\kappa_s - 1}\exp(-s_o x), \tag{17}$$

where $s_o = \frac{R_o^2}{P_s\beta_s}$. By substituting (13) and (17) into (15), the MD probability is given by

$$\mathbb{P}_{\mathrm{MD1}} = \frac{\gamma(\kappa_s, s_w\tau)}{2\Gamma(\kappa_s)} - \frac{s_w^{\kappa_s}}{\pi\Gamma(\kappa_s)}\int_0^{\tau}\int_0^{+\infty} \frac{\sin(v^\delta B - v(\tau - x))}{v\exp(v^\delta C)} x^{\kappa_s - 1}\exp(-s_w x)\mathrm{d}v\mathrm{d}x. \tag{18}$$

Separating the integral with respect to x in (18), we have

$$\begin{aligned}
&\int_0^{\tau} \sin(v^\delta B - v\tau + vx) x^{\kappa_s - 1}\exp(-s_w x)\mathrm{d}x \\
&\overset{(a)}{=} \sin(v^\delta B - v\tau)\int_0^{\tau}\cos(vx)x^{\kappa_s - 1}\exp(-s_w x)\mathrm{d}x + \cos(v^\delta B - v\tau)\int_0^{\tau}\sin(vx)x^{\kappa_s - 1}\exp(-s_w x)\mathrm{d}x \\
&\overset{(b)}{=} \frac{\sin(v^\delta B - v\tau)}{2}\left[(s_w + \mathrm{i}v)^{-\kappa_s}\gamma(\kappa_s, (s_w + \mathrm{i}v)\tau) + (s_w - \mathrm{i}v)^{-\kappa_s}\gamma(\kappa_s, (s_w - \mathrm{i}v)\tau)\right] \\
&\quad + \frac{\mathrm{i}\cos(v^\delta B - v\tau)}{2}\left[(s_w + \mathrm{i}v)^{-\kappa_s}\gamma(\kappa_s, (s_w + \mathrm{i}v)\tau) - (s_w - \mathrm{i}v)^{-\kappa_s}\gamma(\kappa_s, (s_w - \mathrm{i}v)\tau)\right] \\
&= \frac{\Upsilon(v) + \Upsilon^*(v)}{2},
\end{aligned} \tag{19}$$

where step (a) follows from trigonometric functions and step (b) follows from the equation [35, Eqs. (3.944.1) and (3.944.3)]. Combining with (18), we obtain the probability of MD for Willie in FDM as

$$\mathbb{P}_{\mathrm{MD1}} = \frac{\gamma(\kappa_s, s_w\tau)}{2\Gamma(\kappa_s)} - \frac{s_w^{\kappa_s}}{2\pi\Gamma(\kappa_s)}\int_0^{+\infty} \frac{\Upsilon(v) + \Upsilon^*(v)}{v\exp(v^\delta C)}\mathrm{d}v. \tag{20}$$

By summing $\mathbb{P}_{\mathrm{FA}}$ and $\mathbb{P}_{\mathrm{MD1}}$, we can obtain the covert probability in FDM.

Then, we further derive the mathematical expression of connection probability in the following.

Theorem 2. Letting $\zeta = \frac{1}{2^{R_{\mathrm{T}}}-1}$, the connection probability for Bob in FDM is

$$\mathbb{P}_{\mathrm{con1}} = \frac{1}{2} - \frac{1}{\pi}\int_0^{+\infty} \frac{1}{v\exp(v^\delta C)} \frac{\sin(v^\delta B - \kappa_s \arctan(\zeta v/s_b))}{\left(1+(\zeta v/s_b)^2\right)^{\kappa_s/2}}\mathrm{d}v. \tag{21}$$

Proof. Similar to the derivation of MD, the connection probability based on (7) is given by

$$\begin{aligned}
\mathbb{P}_{\mathrm{con1}} &= \mathbb{P}(\log_2(\mathrm{SIR}_b + 1) \geqslant R_{\mathrm{T}}) \\
&= \mathbb{P}(I_b \leqslant \zeta S_b) = \mathbb{E}_{S_b}\left[F_{I_b}(\zeta S_b)\right] \\
&= \frac{1}{2} - \frac{1}{\pi\Gamma(\kappa_s)}\int_0^{\infty}\int_0^{+\infty} \frac{\sin(v^\delta B - \zeta x v/s_b)}{v\exp(v^\delta C)} x^{\kappa_s - 1}\exp(-x)\mathrm{d}x\mathrm{d}v \\
&\overset{\text{(b)}}{=} \frac{1}{2} - \frac{1}{\pi}\int_0^{+\infty} \frac{1}{v\exp(v^\delta C)} \frac{\sin(v^\delta B - \kappa_s \arctan(\zeta v/s_b))}{\left(1+(\zeta v/s_b)^2\right)^{\kappa_s/2}}\mathrm{d}v,
\end{aligned} \tag{22}$$

where step (b) separates the integral about x and applies the formulas [35, Eqs. (3.944.5) and (3.944.6)].

Satellite altitude generally plays an important role in covert satellite communication performance. However, according to Theorems 1 and 2, we can derive a special case where the effect of satellite altitude on connection probability and covert probability can be counteracted by the corresponding change of transmission power in FDM.

Corollary 1. In FDM, if the transmission power P_s can change correspondingly, R_o has no impact on the performance metrics, including covert probability, connection probability, and covert throughput. Specifically, when R_o is multiplied by k, covert throughput will remain constant if P_s can be multiplied by k^2 correspondingly.

Proof. As observed in (11) and (21), R_o and P_s can be regarded as a joint variable $s_o = \frac{R_o^2}{P_s\beta_s}$. As long as s_o remains constant, the covert probability, connection probability, and covert throughput remain unchanged. Thus, the system performance will not be affected by R_o if the requirement on P_s is satisfied.

3.2 MDM

In this subsection, we investigate the performance of the proposed MDM. Referring to Figure 1, the satellite moves from the initial position A to its final destination A' while communicating with Bob, which incorporates the actual trajectory of satellites into the analysis. Meanwhile, the moving trajectory from A to O_1 has the equivalent performance to that from O_1 to A' due to the symmetry motion trajectory. Thus, we only consider the covert performance of the moving trajectory from A to O_1 for convenience.

Since R_o varies with the satellite's position, it is hard to obtain the performance directly, which encourages us to apply the idea of calculus and derive it indirectly. Specifically, we divide the moving satellite trajectory into countless small intervals and assume that there exists a negligible change in position between adjacent intervals. It is reasonable to assume that the intervals are special static scenarios suited at different fixed locations in $\mathcal{A}_{\mathrm{vis}}$. We can obtain the corresponding performance by averaging the countless static scenario performance. We first present the relationship among the distance R_o between A_1 and the terrestrial node o, the moving speed v, and the moving time t.

Lemma 1. As the satellite moves along the orbit from its initial point A, the relationship among R_o, v, and t is

$$R_o^2 = R_{\mathrm{e}}^2 + (R_{\mathrm{e}} + R_{\min})^2 - 2R_{\mathrm{e}}\Big(R_{\mathrm{e}}\cos\Big(\frac{vt}{R_{\mathrm{e}}+R_{\min}}\Big) + \sqrt{2R_{\mathrm{e}}R_{\min} + R_{\min}^2}\sin\Big(\frac{vt}{R_{\mathrm{e}}+R_{\min}}\Big)\Big). \tag{23}$$

Proof. Referring to Figure 1, we have

$$\theta_2 = \frac{vt}{R_{\mathrm{e}}+R_{\min}}, \theta_{\max} = \arccos\Big(\frac{R_{\mathrm{e}}}{R_{\mathrm{e}}+R_{\min}}\Big). \tag{24}$$

Due to the fact that $\theta_1 = \theta_{\max} - \theta_2$, we express the cosine of θ_1 as

$$\cos\theta_1 = \frac{1}{R_{\mathrm{e}}+R_{\min}}\Big(R_{\mathrm{e}}\cos\Big(\frac{vt}{R_{\mathrm{e}}+R_{\min}}\Big) + \sqrt{2R_{\mathrm{e}}R_{\min} + R_{\min}^2}\sin\Big(\frac{vt}{R_{\mathrm{e}}+R_{\min}}\Big)\Big). \tag{25}$$

By the Law of Cosines, the distance between the terrestrial node and the satellite in MDM is

$$R_o(\theta_1) = R_{\rm e}^2 + (R_{\rm e} + R_{\min})^2 - 2R_{\rm e}\,(R_{\rm e} + R_{\min})\cos\theta_1. \tag{26}$$

By substituting (25) into (26), we establish the relationship between R_o, t, and v.

According to Lemma 1, we can obtain the time-average covert probability and connection probability for MDM, given by

$$\xi_2 = \frac{1}{t_{\max}} \int_0^{t_{\max}} \xi_1\left(R_w\left(\theta_1\right)\right) {\rm d}t, \tag{27a}$$

$$\mathbb{P}_{\rm con2} = \frac{1}{t_{\max}} \int_0^{t_{\max}} \mathbb{P}_{\rm con1}\left(R_b\left(\theta_1\right)\right) {\rm d}t, \tag{27b}$$

where $\xi_1\left(R_o\left(\theta_1\right)\right)$ and $\mathbb{P}_{\rm con1}\left(R_o\left(\theta_1\right)\right)$ result from replacing R_o with $R_o\left(\theta_1\right)$ in ξ_1 and $\mathbb{P}_{\rm con1}$. $t_{\max}$ is the moving time from A to O_1.

Lemma 2. The speed v has no impact on time-averaged covert probability and connection probability for MDM.

Proof. For an arbitrary function $f(x)$, the time-average value with respect to $R_o(\theta_1)$ over the moving trajectory from A to O_1 is

$$\begin{aligned} \frac{1}{t_{\max}} \int_0^{t_{\max}} f\left(R_o\left(\theta_1\right)\right) {\rm d}t &\overset{\rm (a)}{=} \frac{1}{t_{\max}} \int_0^{t_{\max}} f\Big(R_o\Big(\theta_{\max} - \frac{vt}{R_{\rm e} + R_{\min}}\Big)\Big) {\rm d}t \\ &\overset{\rm (b)}{=} \frac{1}{\theta_{\max}} \int_0^{\theta_{\max}} f(R_o(\theta)) {\rm d}\theta, \end{aligned} \tag{28}$$

where $t_{\max}$ is the moving time from A to O_1, step (a) follows $\theta_1 = \theta_{\max} - \frac{vt}{R_{\rm e}+R_{\min}}$, and step (b) follows the variable transformation. From (28), when $f(x)$ is known, its average performance is solely determined by $\theta_{\max}$, which is only influenced by $R_{\min}$. It is obvious that for MDM, both covert probability and connection probability are average values with respect to $R_o(\theta_1)$. Thus, we obtain the above result.

This lemma may seem counterintuitive. However, unchanged spatial properties and time-averaging operations can compensate for the effects of the change of v. Specifically, a lower v results in a larger $t_{\max}$, increasing the total received signal energy at terrestrial devices. However, after time-average operations, the average received energy remains unchanged.

Based on Theorem 1, Theorem 2, and Lemma 2, we can conclude the following two corollaries about the covertness and connection performance of MDM.

Corollary 2. The average covert probability for Willie in MDM is expressed as

$$\xi_2 = \frac{1}{2} + \frac{1}{\pi} \int_0^{+\infty} \frac{\sin(v^\delta B - v\tau)}{v\exp(v^\delta C)} {\rm d}v + \frac{1}{\theta_{\max}} \int_0^{\theta_{\max}} \mathbb{P}_{\rm MD1}\left(R_w(\theta)\right) {\rm d}\theta. \tag{29}$$

Proof. Based on (27a), we obtain

$$\xi_2 = \frac{1}{2} + \frac{1}{\pi} \int_0^{+\infty} \frac{\sin(v^\delta B - v\tau)}{v\exp(v^\delta C)} {\rm d}v + \frac{1}{t_{\max}} \int_0^{t_{\max}} \mathbb{P}_{\rm MD1}\left(R_w(\theta_1)\right) {\rm d}\theta. \tag{30}$$

Combining (18) and Lemma 2, the time-average MD probability is expressed as

$$\mathbb{P}_{\rm MD2} = \frac{1}{\theta_{\max}} \int_0^{\theta_{\max}} \mathbb{P}_{\rm MD1}\left(R_w\left(\theta\right)\right) {\rm d}\theta. \tag{31}$$

Similar to FDM, the result can be achieved by summing $\mathbb{P}_{\rm FA}$ and $\mathbb{P}_{\rm MD2}$.

Corollary 3. The time-average connection probability for Willie in MDM is expressed as

$$\mathbb{P}_{\rm con2} = \frac{1}{\theta_{\max}} \int_0^{\theta_{\max}} \mathbb{P}_{\rm con1}\left(R_b\left(\theta\right)\right) {\rm d}\theta. \tag{32}$$

Proof. Similar to Corollary 2.

3.3 SDM

In SDM, the satellite is randomly distributed in $\mathcal{A}_{\text{vis}}$, which causes R_o to be a random variable. We derive both covert probability and connection probability via firstly presenting the PDF of the received signal $S_o = P_s g_o R_o^{-2}$.

Lemma 3. In SDM, the PDF of received signal power S_o is $f_{S_o}(x) = \frac{1}{x^2}\Psi(x)$ where $s_{\max} = \frac{R_{\max}^2}{\beta P_s}$, $s_{\min} = \frac{R_{\min}^2}{\beta P_s}$, and $\Psi(x) = \frac{\kappa_s \beta P_s}{R_{\max}^2 - R_{\min}^2} \frac{1}{\Gamma(\kappa_s+1)} \left[\gamma(\kappa_s+1, s_{\max}x) - \gamma(\kappa_s+1, s_{\min}x)\right]$.

Proof. The proof is given in Appendix A.

Moreover, since FDM is the fundamental model, we can obtain the corresponding expressions of covert probability and connection probability in SDM with the similar derivations of Theorems 1 and 2, which are presented in the following two corollaries.

Corollary 4. The covert probability for Willie in SDM is expressed as

$$\xi_3 = \frac{1}{2} + \frac{1}{\pi}\int_0^{+\infty} \frac{\sin(v^\delta B - v\tau)}{v\exp(v^\delta C)}\mathrm{d}v + \frac{1}{2}\int_0^{\tau} \frac{\Psi(x)}{x^2}\mathrm{d}x - \frac{1}{\pi}\int_0^{\tau}\int_0^{+\infty} \frac{\sin(v^\delta B - v(\tau-x))}{v\exp(v^\delta C)}\frac{\Psi(x)}{x^2}\mathrm{d}v\mathrm{d}x. \quad (33)$$

Proof. Similar to Theorem 1, we derive the probability expression of MD for SDM, given by

$$\mathbb{P}_{\text{MD3}} = \frac{1}{2}\int_0^{\tau} \frac{1}{x^2}\Psi(x)\,\mathrm{d}x - \frac{1}{\pi}\int_0^{\tau}\int_0^{+\infty} \frac{\sin(v^\delta B - v(\tau-x))}{v\exp(v^\delta C)}\frac{1}{x^2}\Psi(x)\,\mathrm{d}v\mathrm{d}x. \quad (34)$$

Then, the result can be achieved by summing the previously derived $\mathbb{P}_{\text{FA}}$ and the above formula $\mathbb{P}_{\text{MD3}}$.

Corollary 5. The connection probability for Willie in SDM is expressed as

$$\mathbb{P}_{\text{con3}} = \frac{1}{2} - \frac{1}{\pi}\int_0^{+\infty}\int_0^{+\infty} \frac{\sin(v^\delta B - \zeta v x)}{v\exp(v^\delta C)}\frac{1}{x^2}\Psi(x)\,\mathrm{d}v\mathrm{d}x. \quad (35)$$

Proof. Similar to Theorem 2.

4 Covert throughput analysis

Considering the covert requirement and limited transmission power, we can formulate the following optimization problem to obtain the optimal covert throughput, given by

$$\begin{aligned} \max_{R_{\text{T}}, P_s} \quad & \mathbb{P}_{\text{con}i}(R_{\text{T}}, P_s) R_{\text{T}}, \\ \text{s.t.} \quad & \xi_i^*(P_s) \geqslant 1-\varepsilon, \\ & P_s \leqslant P_{\max}, \end{aligned} \quad (36)$$

where $i \in \{1,2,3\}$ represents the different network models and $P_{\max}$ is maximum satellite transmission power. By observing (36), the constraint conditions are solely affected by P_s. Thus, we can simplify the constraints by limiting P_s within a specific range while satisfying all constraint conditions.

Since the increase of transmission power P_s will lead to the decrease of covert probability, P_s and ξ are inversely related [17]. Assuming that there exists $P_{\max i}$ such that $\xi_i^*(P_{\max i}) = 1-\varepsilon$, it can be deduced that when $P_s \leqslant P_{\max i}$, ξ will always be greater than $1-\varepsilon$. Therefore, the covertness constraint can be transformed into the power constraint, and we can reformulate (36) as

$$\begin{aligned} \max_{R_{\text{T}}, P_s} \quad & \mathbb{P}_{\text{con}i}(R_{\text{T}}, P_s) R_{\text{T}}, \\ \text{s.t.} \quad & P_s \leqslant \min\{P_{\max}, P_{\max i}\}. \end{aligned} \quad (37)$$

Since the connection probability $\mathbb{P}_{\text{con}i}$ and P_s are positively related, the optimal transmission power is $P_{S_i}^* = \min\{P_{\max}, P_{\max i}\}$, and the optimization problem can be simplified as

$$\max_{R_{\text{T}}} \quad \mathbb{P}_{\text{con}i}\left(R_{\text{T}}, P_{S_i}^*\right) R_{\text{T}}. \quad (38)$$

For (38), the optimization problem only consists of a singular objective function without any constraints, and the objective function contains only one optimization variable R_{T}. Thus, we can employ the one-dimensional search to obtain the optimal R_{T} and determine the optimal covert throughput.

Table 1 Symbol descriptions and default parameters.

Symbol	Description	Default value
R_{e}	Earth radius	6371 km
$R_{\min}$	Altitude of satellite	1000 km
λ_{I}	Density of terrestrial interference	10^{-5}
P_{I}	Transmission power of terrestrial interference	15 dBm
α	Terrestrial path loss exponent	4
P_s	Satellite transmission power	45 dBm
b_0, m, Ω	Shadowed Rician fading: infrequent light shadowing	$0.158, 19.4, 1.29$
ε	Covert requirement	0.1

5 Numerical results

In this section, we present the simulations to verify the derived expressions and covert throughput for the three network models. The terrestrial simulation region is set to $[-L, L]^2$ where $L = 5$ km and the interference nodes following a PPP are randomly and uniformly distributed within the square region. Monte Carlo is employed to validate the theoretical expressions of connection probability and covert probability. The simulation times exceed 10000. Additionally, we investigate the impact of various SR channel parameters on covert communication performance: infrequent light shadowing (ILS) $\{b_0 = 0.158, m = 19.4, \Omega = 1.29\}$, average shadowing (AS) $\{b_0 = 0.126, m = 10.1, \Omega = 0.835\}$, and frequent heavy shadowing (FHS) $\left\{b_0 = 0.063, m = 0.739, \Omega = 8.97 \times 10^{-4}\right\}$ [30,31]. The default parameter values for the three network models are presented in Table 1.

5.1 Validation for the derived expressions

Figure 2 illustrates the relationship between connection probability $\mathbb{P}_{\mathrm{con}}$ and transmission rate threshold R_{T} with $P_{\mathrm{I}} = 10$ dBm for the three network models. It is evident that the simulation results closely match the theoretical results, which validate the derived expressions. Meanwhile, we can obtain $\mathbb{P}_{\mathrm{con1}} > \mathbb{P}_{\mathrm{con2}} > \mathbb{P}_{\mathrm{con3}}$ for the three models. FDM has the best connection performance since the satellite is always directly above Bob, located at the closest transmission position in $\mathcal{A}_{\mathrm{vis}}$, which results in the highest received signal power at terrestrial Bob in three models. According to Lemma 3, the PDF of the distance R_b between the satellite and terrestrial node for SDM, we can obtain $f_R(R_1) < f_R(R_2)$ if $R_{\min} < R_1 < R_2 < R_{\max}$. It means the probability of the satellite being at the near communication positions (NCP) is lower than at the far communication positions (FCP) in $\mathcal{A}_{\mathrm{vis}}$ and the satellite tends to be located at FCP. For MDM, the performance from the initial position to the final destination of the satellite trajectory in $\mathcal{A}_{\mathrm{vis}}$ is considered in a comprehensive average manner with equal probabilities of being at the NCP or FCP. Based on the above analysis, the performance of MDM and SDM essentially is the average performance of the corresponding FDM ($R_{\min} < R_o < R_{\max}$) with different average manners. However, R_b is distributed in $[R_{\min}, R_{\max}]$ with the same probability in MDM, while distributed in second half of $[R_{\min}, R_{\max}]$ with the greater probability in SDM. Therefore, from a statistical view, MDM has higher average signal power than SDM, resulting in better reliability.

Figure 3 shows the relationship between the covert probability ξ and different detection thresholds τ for the three models. We can observe that ξ first decreases and then rises as τ increases. When τ is low, the detector sensitivity is high and Willie will be highly alert to minor changes in the received signal, thereby increasing the probability of FA. Conversely, when τ is high, the detector sensitivity is low and Willie may be unaware of the occurrence of the signal transmission, thereby increasing the probability of MD. Thus, Willie has the optimal τ minimizing the occurrences of FA and MD and achieves the lowest ξ. It can be observed that in contrast to $\mathbb{P}_{\mathrm{con}}$, ξ follows $\xi_1 < \xi_2 < \xi_3$, which means that FDM has the worst covertness while SDM has the best one. This is because ξ is inversely correlated to the received signal power while $\mathbb{P}_{\mathrm{con}}$ is positively correlated to that. When the transmission signal power is sufficiently large, it is harder to conceal Alice's signal in the terrestrial interference signals, making it easier to be detected by Willie and thus reducing its covertness. Meanwhile, we can observe that different models have different optimal detection thresholds, which suggests that it is essential to account for the change of optimal detection threshold when studying different models.

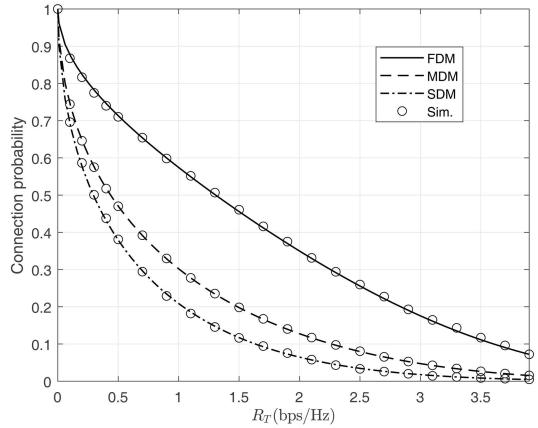

Figure 2 Connection probability versus transmission rate threshold for three network models.

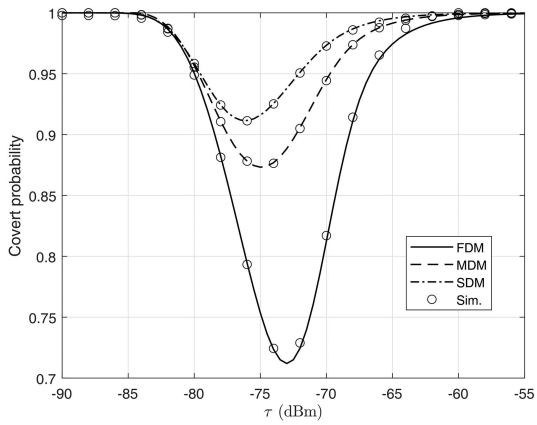

Figure 3 Covert probability versus detection threshold for three network models.

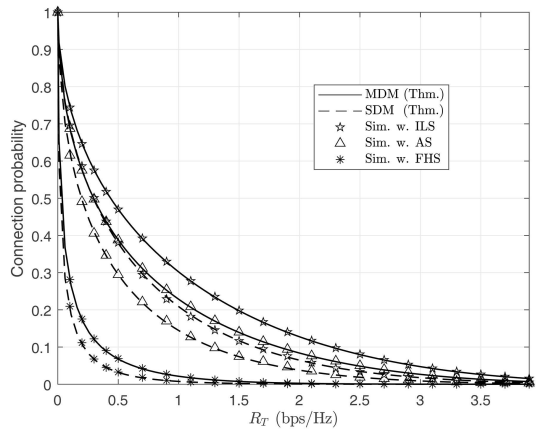

Figure 4 Connection probability versus transmission rate threshold with different SR parameters for MDM and SDM.

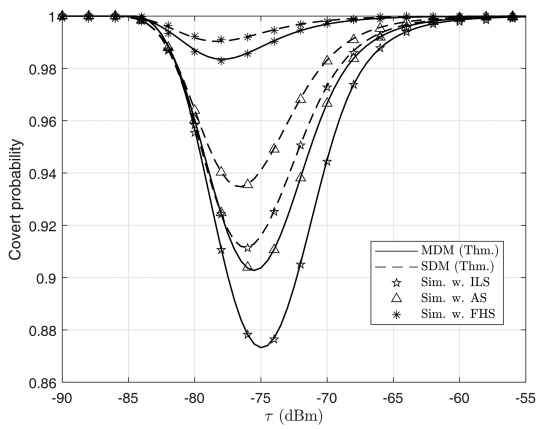

Figure 5 Covert probability versus detection threshold with different SR parameters for MDM and SDM.

5.2 Effect of different parameters for MDM and SDM

Figure 4 shows the impact of different SR parameters on the connection probability $\mathbb{P}_{\text{con}}$ in MDM and SDM. It can be observed that $\mathbb{P}_{\text{con}}$ in MDM is still higher than that in SDM under the same SR parameters, which further proves the above analysis about $\mathbb{P}_{\text{con}}$ of MDM and SDM in Figure 2. Comparing FHS, AS, and ILS, we can conclude that severe channel shadowing will decrease the power of the transmission signal, leading to lower received signal power and reducing $\mathbb{P}_{\text{con}}$ for Bob.

Figure 5 shows the impact of different SR parameters on the covert probability ξ in MDM and SDM. In contrast to Figure 4, severe channel shadowing will introduce more channel uncertainty at Willie, which makes the transmission signal concealed in terrestrial interference more easily and improves the covertness. Thus, the more severe channel shadowing will contribute to better covertness.

Figure 6 illustrates the impact of satellite altitude $R_{\min}$ with different transmission power P_s on covert probability ξ and connection probability $\mathbb{P}_{\text{con}}$ under the fixed transmission rate threshold $R_{\text{T}} = 0.5$ bps/Hz in MDM and SDM. Since Willie can obtain the optimal detection threshold based on the known parameters, we select it as the detection threshold. We can observe from both figures and conclude that MDM and SDM have similar trends on ξ and $\mathbb{P}_{\text{con}}$ with respect to $R_{\min}$. It can also be observed that the trends of ξ and $\mathbb{P}_{\text{con}}$ are completely opposite, which is similar to the above analysis that the stronger signal will be beneficial to $\mathbb{P}_{\text{con}}$ and detrimental to ξ by decreasing the environment uncertainty. As $R_{\min}$ increases, the communication distance between Alice and terrestrial nodes will also increase, leading to greater path loss and reducing transmission signal power significantly. Thus, the higher $R_{\min}$ will lead to the better ξ but worse $\mathbb{P}_{\text{con}}$. And the increase of P_s will enhance the received signal power at terrestrial

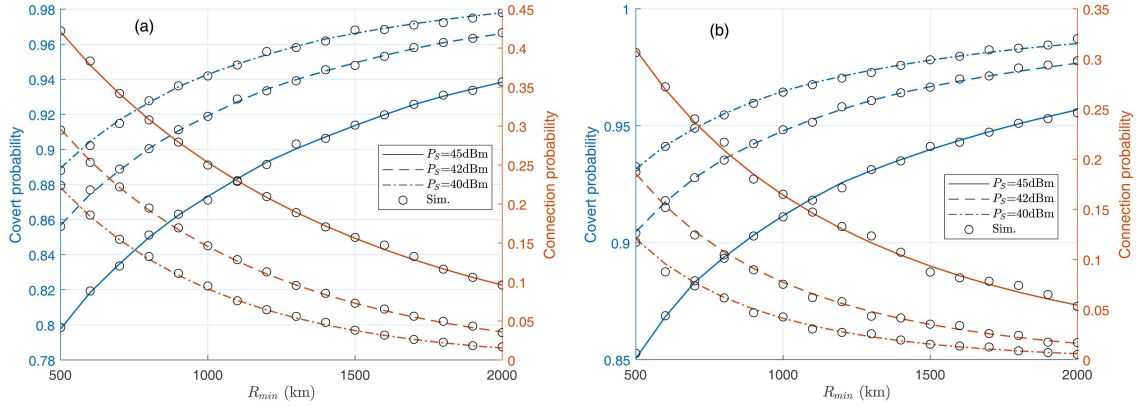

Figure 6 (Color online) Covert probability and connection probability versus altitude with different transmission power. (a) MDM; (b) SDM.

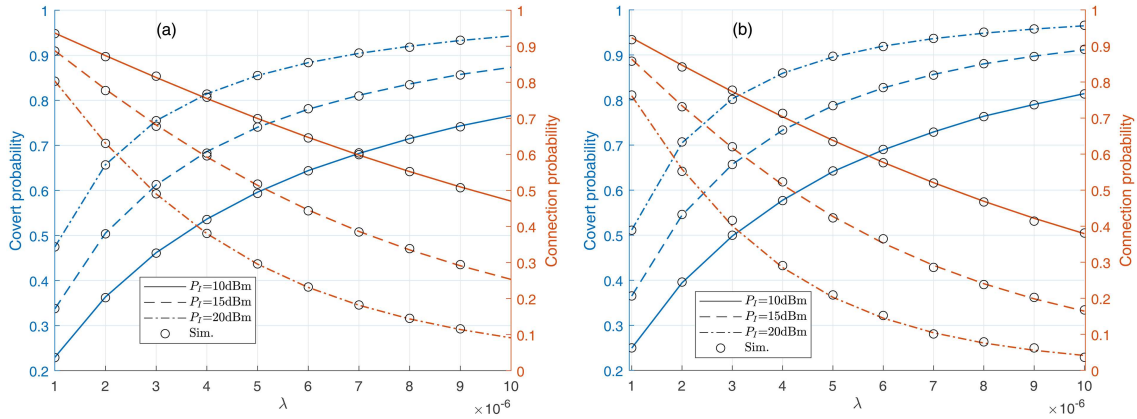

Figure 7 (Color online) Covert probability and connection probability versus interference density with different interference transmission power. (a) MDM; (b) SDM.

nodes, which means the higher P_s will lead to better $\mathbb{P}_{\text{con}}$ but worse ξ.

Figure 7 shows the impact of the terrestrial interference density λ_{I} and power P_{I} on covert probability ξ and connection probability $\mathbb{P}_{\text{con}}$ under transmission rate threshold $R_{\text{T}} = 0.5$ bps/Hz in MDM and SDM. Similarly, we select the optimal detection threshold under different parameters as detection threshold. Although Figures 7(a) and (b) have similar trends to Figures 6(a) and (b), the underlying reasons for this trend are entirely different from those in the former figures. The increase of λ_{I} will rise the number of interference nodes, thereby resulting in the higher total received interference signal power at Bob, which makes it more difficult for Bob and Alice to establish the connection link and reduces $\mathbb{P}_{\text{con}}$. However, this will make the signal of Alice more easily concealed within the interference and increase the difficulty of detection by Willie, thereby enhancing ξ. Although the number of interference nodes does not rise with a higher P_{I}, ξ will increase and $\mathbb{P}_{\text{con}}$ will decrease due to the enhancement of the total interference signal power.

5.3 Covert throughput for MDM and SDM

Figure 8 illustrates the impact of satellite altitude $R_{\min}$ on the covert throughput η for different interference density λ_{I} and SR parameters in MDM and SDM. We first observe that MDM and SDM have similar performance and behave closely. The reason for this phenomenon is that MDM and SDM are both extended from FDM. However, these two models are totally different: MDM considers the mobility based on FDM, while SDM accounts for the position uncertainty. Then, it can be observed that the trend of η shows a slight decline when $\lambda_{\text{I}} = 10^{-6}$, but a dramatic decline when $\lambda_{\text{I}} = 10^{-5}$ as $R_{\min}$ increases. Meanwhile, there exists a small overlap when $R_{\min}$ is low. The main reason for this phenomenon is different transmission power. Specifically, the former considers $P_{\max i}$ as the transmission power, while the latter employs $P_{\max}$. We first analyze the causes of the slight decline. According to Corollary 1,

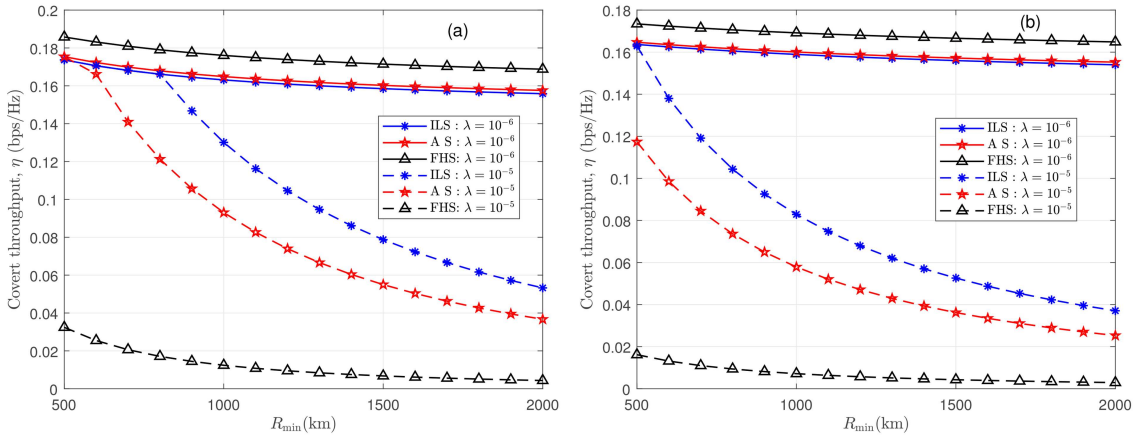

Figure 8 (Color online) Covert throughput versus altitude with different SR parameters and interference density. (a) MDM; (b) SDM.

we can obtain that R_o has no effect on η if Alice has sufficiently large transmission power P_s. Thus, η will remain constant with the increase of R_o if $P_{\max_1} < P_{\max}$, while be reduced if $P_{\max 1} > P_{\max}$. When $R_{\min}$ increases, the part of decreased η will expand while the part of constant η will shrink in the range of $[R_{\min}, R_{\max}]$. Since MDM and SDM are the averages of FDM over $[R_{\min}, R_{\max}]$, a slight decline will appear when $R_{\min}$ increases. Meanwhile, since there is part of unchanged η, where $P_{\max 1} < P_{\max}$, the optimal power $P_{\max 2}$ is less than $P_{\max}$ and is used as the transmission power. The dramatic decline is because $P_{\max i} > P_{\max}$ and $P_{\max}$ as the transmission power. The overlap for different λ_{I} occurs because the optimal power $P_{\max i}$ is used as the transmission power. Figure 8(b) has a similar trend to Figure 8(a) but fewer overlapping regions. Based on the above analysis, we can obtain that SDM has better covertness than MDM, which means $P_{\max 3} > P_{\max 2}$ when the covert requirement is exactly met. Thereby, $P_{\max 3}$ earlier achieved the maximum power $P_{\max}$ and the less overlap will appear compared MDM.

6 Conclusion

In this paper, we investigated the performance of satellite-terrestrial covert communication, where terrestrial Bob receives covert signals from the satellite while being affected by the terrestrial interference nodes following a PPP and simultaneously preventing the detection by terrestrial Willie. Moreover, we mainly focused on three network models: the satellite in a fixed position, the satellite moving along its orbit, and the satellite randomly distributed in $\mathcal{A}_{\mathrm{vis}}$. Specifically, we derived the analytical expressions of FA, MD, and connection probability for three models. Then, we formulated an optimization problem to obtain the covert throughput, which can be simplified by analyzing the relationship between the optimization variables and constraints and can be solved by applying one-dimensional search. We concluded that the satellite altitude does not affect the covert performance of FDM. Then, we validated the derived expressions through simulations. Meanwhile, numerical results indicated that, compared with MDM, SDM tends to be located at far communication positions under the same parameter conditions, resulting in worse reliability but better covertness. In summary, with the proposed three network models and the corresponding analytical results, theoretical insights can be provided for the performance analysis on realistic satellite-terrestrial covert communication models and analytically tractable ones.

Acknowledgements This work was supported in part by National Natural Science Foundation of China (Grant Nos. 62371086, 62171154, 62201115), Natural Science Foundation of Liaoning Province (Grant No. 2023-MSBA-015), and Fundamental Research Funds for the Central Universities (Grant No. DUT24MS015).

References

1 Al-Hraishawi H, Chougrani H, Kisseleff S, et al. A survey on nongeostationary satellite systems: the communication perspective. IEEE Commun Surv Tut, 2023, 25: 101–132
2 Wang R, Kishk M A, Alouini M S. Ultra-dense LEO satellite-based communication systems: a novel modeling technique. IEEE Commun Mag, 2022, 60: 25–31
3 Sheng M, Zhou D, Bai W, et al. Coverage enhancement for 6G satellite-terrestrial integrated networks: performance metrics, constellation configuration and resource allocation. Sci China Inf Sci, 2023, 66: 130303
4 Xu L, Jiao J, Jiang S Y, et al. Semantic-aware coordinated transmission in cohesive clustered satellites: utility of information perspective. Sci China Inf Sci, 2024, 67: 199301

5 Wang S, Ye J, Chen C, et al. Safeguarding inter-satellite transmissions: a viewpoint from covertness. IEEE Wireless Commun, 2025, 32: 221–228
6 An J, Kang B, Ouyang Q, et al. Covert communications meet 6G NTN: a comprehensive enabler for safety-critical IoT. IEEE Netw, 2024, 38: 17–24
7 Yue P, An J, Zhang J, et al. Low earth orbit satellite security and reliability: issues, solutions, and the road ahead. IEEE Commun Surv Tut, 2023, 25: 1604–1652
8 Yan S, Zhou X, Hu J, et al. Low probability of detection communication: opportunities and challenges. IEEE Wireless Commun, 2019, 26: 19–25
9 Jiang Y E, Wang L, Chen H H, et al. Physical layer covert communication in B5G wireless networks its research, applications, and challenges. Proc IEEE, 2024, 112: 47–82
10 Chen W Y, Ding H Y, Wang S L, et al. Beamforming design for covert broadcast communication with hidden adversary. Sci China Inf Sci, 2024, 67: 162304
11 Jiang X, Chen X, Tang J, et al. Covert communication in UAV-assisted air-ground networks. IEEE Wireless Commun, 2021, 28: 190–197
12 Chen X, An J, Xiong Z, et al. Covert communications: a comprehensive survey. IEEE Commun Surv Tut, 2023, 25: 1173–1198
13 Bash B A, Goeckel D, Towsley D. Limits of reliable communication with low probability of detection on AWGN channels. IEEE J Sel Areas Commun, 2013, 31: 1921–1930
14 Lee S, Baxley R J, Weitnauer M A, et al. Achieving undetectable communication. IEEE J Sel Top Signal Process, 2015, 9: 1195–1205
15 He B, Yan S, Zhou X, et al. On covert communication with noise uncertainty. IEEE Commun Lett, 2017, 21: 941–944
16 Sobers T V, Bash B A, Guha S, et al. Covert communication in the presence of an uninformed jammer. IEEE Trans Wireless Commun, 2017, 16: 6193–6206
17 He B, Yan S, Zhou X, et al. Covert wireless communication with a Poisson field of interferers. IEEE Trans Wireless Commun, 2018, 17: 6005–6017
18 Jiang Y, Wang L, Chen H H. Covert communications with randomly distributed adversaries in wireless energy harvesting enabled D2D underlaying cellular networks. IEEE Trans Inform Forensic Secur, 2023, 18: 5401–5415
19 Ma R, Yang W, Guan X, et al. Covert mmWave communications with finite blocklength against spatially random wardens. IEEE Internet Things J, 2024, 11: 3402–3416
20 Zhao J, Li G, Chen G, et al. Covert communication of IRS-assisted wireless networks with stochastic geometry approach. IEEE Wireless Commun Lett, 2024, 13: 974–978
21 Wang Q, Guo S, Wu C, et al. STAR-RIS aided covert communication in UAV air-ground networks. IEEE J Sel Areas Commun, 2025, 43: 245–259
22 Wang C, Xiong Z, Zheng M, et al. Covert communications via two-way IRS with noise power uncertainty. IEEE Trans Commun, 2024, 72: 4803–4815
23 Wu Y, Chen X, Liu M, et al. IRS-assisted covert communication with equal and unequal transmit prior probabilities. IEEE Trans Commun, 2024, 72: 2897–2912
24 Wang M, Xia B, Yao Y, et al. Fundamental limit among covertness, reliability, latency and throughput for IRS-enabled short-packet communications. IEEE Trans Wireless Commun, 2024, 23: 3886–3900
25 Zhang J, Wang W, Gao Y, et al. Robust covert multicasting aided by STAR-RIS with hardware impairment. IEEE Trans Wireless Commun, 2024, 23: 16172–16186
26 Yang F, Wang C, Xiong J, et al. UAV-enabled robust covert communication against active wardens. IEEE Trans Veh Technol, 2024, 73: 9159–9164
27 Jiao L, Chen X, Xu L, et al. UAV-relayed finite-blocklength covert communication with channel estimation. IEEE Trans Veh Technol, 2024, 73: 9032–9037
28 Okati N, Riihonen T, Korpi D, et al. Downlink coverage and rate analysis of low Earth orbit satellite constellations using stochastic geometry. IEEE Trans Commun, 2020, 68: 5120–5134
29 Wang X, Deng N, Wei H. Coverage and rate analysis of LEO satellite-to-airplane communication networks in terahertz band. IEEE Trans Wireless Commun, 2023, 22: 9076–9090
30 Jung D H, Ryu J G, Byun W J, et al. Performance analysis of satellite communication system under the Shadowed-Rician fading: a stochastic geometry approach. IEEE Trans Commun, 2022, 70: 2707–2721
31 Talgat A, Kishk M A, Alouini M S. Stochastic geometry-based uplink performance analysis of IoT over LEO satellite communication. IEEE Trans Aerosp Electron Syst, 2024, 60: 4198–4213
32 Song D, Yang Z, Pan G, et al. RIS-assisted covert transmission in satellite C terrestrial communication systems. IEEE Internet Things J, 2023, 10: 19415–19426
33 Feng S, Lu X, Sun S, et al. Covert communication in large-scale multi-tier LEO satellite networks. IEEE Trans Mobile Comput, 2024, 23: 11576–11587
34 Abdi A, Lau W C, Alouini M, et al. A new simple model for land mobile satellite channels: first- and second-order statistics. IEEE Trans Wireless Commun, 2003, 2: 519–528
35 Gradshteyn I S, Ryzhik I M. Table of Integrals, Series, and Products. Pittsburgh: Academic Press, 2014

Appendix A Proof of Lemma 3

Based on the previous work [28, 30], we employ the derived CDF of $\bar{R}$ directly, where $\bar{R}$ denotes the distance between the satellite and the terrestrial node when the satellite is randomly distributed in the whole visible sphere surface. The CDF of $\bar{R}$ is

$$F_{\bar{R}}(x) = \frac{x^2 - R_{\min}^2}{4R_{\mathrm{e}}(R_{\mathrm{e}} + R_{\min})}. \tag{A1}$$

The formula of (A1) describes the statistical properties wherein the satellite is randomly distributed in the whole orbit, which cannot be directly applied to SDM as this model assumes that the satellite is randomly distributed in $\mathcal{A}_{\mathrm{vis}}$. However, $\mathcal{A}_{\mathrm{vis}}$ is a part of the moving orbit, and we can apply the definition of conditional probability to derive the CDF of R_o, given by

$$F_{R_o}(x) = \mathbb{P}(R_o \leqslant x) = \frac{\mathbb{P}(\bar{R} \leqslant x, \bar{R} \leqslant R_{\max})}{\mathbb{P}(\bar{R} \leqslant R_{\max})} = \frac{x^2 - R_{\min}^2}{R_{\max}^2 - R_{\min}^2}. \tag{A2}$$

Based on the PDF of R_o via taking the derivative of (A2) and the channel fading approximation $g_o \sim \text{Gamma}\,(\kappa_s, \beta_s)$, the CDF of received LEO signal power is

$$\begin{aligned} F_{S_o}(x) &= \mathbb{P}(S_o \leqslant x) = \mathbb{E}_{R_o}\Big[F_{g_o}\Big(\frac{xR_o^2}{P_s}\Big)\Big] \\ &= \frac{1}{\Gamma(\kappa_s)}\left(\int_0^{\frac{xR_{\min}^2}{P_s\beta}} t^{\kappa_s-1}\mathrm{e}^{-t}\mathrm{d}t \int_{R_{\min}}^{R_{\max}} \frac{2r}{R_{\max}^2 - R_{\min}^2}\mathrm{d}r + \int_{\frac{xR_{\min}^2}{P_s\beta}}^{\frac{xR_{\max}^2}{P_s\beta}} t^{\kappa_s-1}\mathrm{e}^{-t} \int_{\sqrt{\frac{P_s\beta t}{x}}}^{R_{\max}} \frac{2r}{R_{\max}^2 - R_{\min}^2}\mathrm{d}r\mathrm{d}t\right) \\ &= \frac{1}{\Gamma(\kappa_s)}\left(\int_0^{\frac{xR_{\min}^2}{P_s\beta}} t^{\kappa_s-1}\mathrm{e}^{-t}\mathrm{d}t + \frac{R_{\max}^2}{R_{\max}^2 - R_{\min}^2}\int_{\frac{xR_{\min}^2}{P_s\beta}}^{\frac{xR_{\max}^2}{P_s\beta}} t^{\kappa_s-1}\mathrm{e}^{-t}\mathrm{d}t - \frac{P_s\beta}{R_{\max}^2 - R_{\min}^2}\frac{1}{x}\int_{\frac{xR_{\min}^2}{P_s\beta}}^{\frac{xR_{\max}^2}{P_s\beta}} t_s^{\kappa}\mathrm{e}^{-t}\mathrm{d}t\right). \end{aligned} \tag{A3}$$

We can obtain the result by taking the derivative of (A3) with respect to x.